Clinical Radiology 74 (2019) 131–139

Contents lists available at ScienceDirect

Clinical Radiology

journal homepage: www.clinicalradiologyonline.net

External validation of ADNEX MR SCORING system: a single-centre retrospective study

K. Sasaguri [a,*], K. Yamaguchi [a], T. Nakazono [a], M. Mizuguchi [a], S. Aishima [b], M. Yokoyama [c], H. Irie [a]

[a] Department of Radiology, Faculty of Medicine, Saga University, Saga, 849-8501, Japan
[b] Department of Pathology and Microbiology, Faculty of Medicine, Saga University, Saga, 849-8501, Japan
[c] Department of Obstetrics & Gynecology, Faculty of Medicine, Saga University, Saga, 849-8501, Japan

ARTICLE INFORMATION

Article history:
Received 9 August 2018
Accepted 31 October 2018

AIM: To evaluate the accuracy of the ADNEX MR SCORING system for characterising adnexal masses.

MATERIALS AND METHODS: An institutional review board approved this retrospective study. The study population comprised 663 women who underwent magnetic resonance imaging (MRI) from January 2007 to December 2014 to characterise 778 adnexal masses that were indeterminate under ultrasonography (590 benign and 188 malignant). Two radiologists independently reviewed the MRI images. The masses were scored from 1 to 5 according to the ADNEX MR SCORING system. The diagnostic performance of the system was evaluated by receiver operating characteristic (ROC) analysis. Masses scored 4 or greater were considered malignant (including tumours of borderline malignancy or low malignant potential).

RESULTS: The malignancy rates of masses with scores of 2, 3, 4 and 5 were 1.9% (8/419), 12.8% (19/149), 62.6% (57/91) and 87.4% (104/119) for reader 1 and 2.1% (9/424), 13.6% (20/147), 67.6% (71/105) and 86.3% (88/102) for reader 2, respectively. The areas under the ROC curves for the differentiation of benign and malignant masses were 0.929 and 0.923, respectively; the sensitivity, specificity and accuracy of diagnosis were 85.6% (161/188), 91.7% (541/590), and 90.2% (702/778) for reader 1 and 84.6% (159/188), 91.9% (542/590), and 90.1% (701/778) for reader 2, respectively. Tumours of borderline malignancy or low malignant potential had a higher rate of misclassification (46.1%) than other malignant tumours (6–7.4%).

CONCLUSION: The ADNEX MR SCORING system was highly accurate in differentiating benign and malignant adnexal masses, although it may be less accurate for tumours of borderline malignancy or low malignant potential.

Introduction

Adnexal masses (masses of the ovary, fallopian tube, or surrounding connective tissues) are a common gynaecological problem. A reliable method with which to differentiate a benign from a malignant adnexal mass would provide a basis for optimal preoperative planning and may

* Guarantor and correspondent: K. Sasaguri, Department of Radiology, Faculty of Medicine, Saga University, 5-1-1 Nabeshima, Saga, 849-8501, Japan. Tel.: +81 952 34 2309; fax: +81 52 34 2016.
E-mail address: k.sasaguri@gmail.com (K. Sasaguri).

https://doi.org/10.1016/j.crad.2018.10.014
0009-9260/

also reduce the number of unnecessary laparotomies performed on patients for benign disease.[1]

Ultrasonography (US) is the first-line imaging study of women clinically suspected to have adnexal masses.[2] For adnexal masses indeterminate under US, magnetic resonance imaging (MRI) is considered to be a useful problem-solving technique. Gadolinium-enhanced MRI appears to be more accurate than US in the assessment of adnexal masses.[3] In addition, functional imaging techniques, including perfusion- and diffusion-weighted imaging (DWI), have recently been shown to increase the diagnostic accuracy of conventional MRI in the differentiation of benign from malignant adnexal masses.[4,5]

In 2013, Thomassin-Naggara *et al.* reported an MRI scoring system (the ADNEX MR SCORING system) designed for use in pelvic MRI, which is performed to characterise adnexal masses that are indeterminate under US.[6] In this system, adnexal masses are classified into five categories according to the likelihood ratio of malignancy. The scoring system was highly reproducible and accurate, yielding an area under the receiver operating characteristic (ROC) curves (AUC) that ranged from 0.943–0.980. Currently, one retrospective validation study performed at a single external centre has been reported,[7] and a prospective multicentre study titled "EURAD-MR classification: European multicenter study (EURAD)" is ongoing.[8] The former study included a relatively small number of cases, and the latter study is being performed at institutions in European countries only. Therefore, additional studies from other regions with large numbers of cases are needed to confirm the accuracy and reliability of the scoring system. The purpose of this study was to evaluate the accuracy of the ADNEX MR SCORING system.

Materials and methods

This study was conducted retrospectively at a 600-bed community teaching hospital according to the STARD guidelines for studies of diagnostic accuracy. The hospital's Institutional Review Board approved the study and waived the requirement for informed consent for this retrospective review of medical records.

The selection of patients was performed according to the method used in the original study.[6] The radiological database was searched retrospectively and all pelvic MRI studies performed in female patients from January 2007 (when the MRI unit described below was installed in the hospital) to December 2014 were retrieved. Then, the request forms for the MRI studies and outpatient records were reviewed to identify patients who underwent MRI to characterise adnexal masses that were indeterminate under US (n=1005). Subsequently, studies were excluded of women evaluated in the course of neoadjuvant chemotherapy (n=23); studies of pregnant women (n=13); studies with technical problems (n=2); studies in which no adnexal lesions or only cysts with the appearance of physiological ovarian cysts <3 cm were present at MRI (n=70); and studies without contrast-enhanced images (n=141). Among the remaining patients, 93 patients had no available standard references (no histopathological diagnosis or imaging follow-up) and were therefore excluded. The final population comprised 663 women with 778 adnexal masses (Fig 1). Five hundred and forty-eight women had one mass, and 115 had multiple masses. The number of masses on MRI per patient was recorded independently by two radiologists blinded to the pathology results: reader 1 with 11 years and reader 2 with 15 years of experience in pelvic MRI. Discordance in the number or laterality of adnexal masses per patient between the two readers was resolved by consensus review.

MRI technique

MRI was performed on a 1.5 or 3 T MRI unit (MAGNETOM Avant or MAGNETOM Trio, Siemens, Erlangen, Germany). A pelvic phased-array coil was used in all patients. Patients fasted for at least 3 hours before MRI and received 1 mg of an antispasmodic drug (unless contraindicated) intramuscularly immediately before MRI to reduce bowel peristalsis. The standard MRI protocol for adnexal mass evaluation includes: axial gradient-echo T1-weighted imaging (WI) with and without fat suppression, axial and sagittal non–fat-suppressed turbo spin-echo T2WI, and axial diffusion WI (DWI) before gadolinium chelate injection. DWI was acquired using a single-shot echo-planar imaging sequence. The b-values corresponding to the diffusion-sensitising gradient were 0 and 1000 s/mm^2. Motion-probing gradient pulses were placed in the three orthogonal planes. Isotropic DWI images were generated using the three orthogonal axis images. Then, axial dynamic contrast-enhanced T1WI was performed through the lesion using a three-dimensional (3D) volumetric interpolated breath-hold sequence. The total acquisition time for this sequence was about 20 seconds. This sequence was performed before and after intravenous injection of 0.1 mmol/kg of gadopentetate dimeglumine at a rate of 2 ml/s for 30,

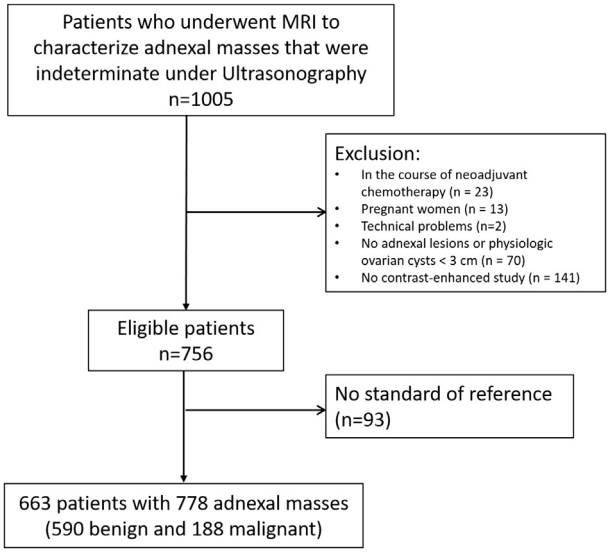

Figure 1 Flowchart of patient selection.

60, 90, 120, and 180 seconds. Subtraction images, in which the precontrast images are digitally subtracted from the post-contrast images, were created when a mass had a high signal intensity area on precontrast images. Finally, delayed contrast-enhanced axial and sagittal T1-weighted spin-echo images were obtained.

MRI image analysis

The two radiologists described above independently reviewed the MRI images. The latest MRI examinations were used for review when multiple follow-up studies were performed, but examinations in the course of neoadjuvant chemotherapy or examinations without contrast enhancement were not used, as described above. The readers knew the purpose of the study but were blinded to the US and clinical findings; however, readers 1 and 2 had experience with 248 patients with 286 masses (36.9% of all masses) and 69 patients with 89 masses (11.5%) in their respective clinical settings prior to this study.

The readers recorded the MRI features used in the ADNEX MR SCORING system according to the definitions in the original report (Table 1). In this system, adnexal masses are scored from 1 to 5 (1: no mass, 2: benign mass, 3: probably benign mass, 4: indeterminate mass, 5: probably malignant mass; Fig 2). Cases with an ADNEX MR score of 1 were excluded from the evaluation as well as the original study.[6]

If there were areas with different scores within the same mass, the higher score was adopted. For example, if an adnexal mass had heterogeneous solid tissue that showed low b=1000 s/mm^2-weighted and low T2-weighted signal intensity within part of the solid tissue, but high signal intensity and curve type 3 enhancement in another part, the mass was scored as a 5. Case examples of the time–signal-intensity curve analyses are shown in Figs 3–5.

When a patient had masses within the bilateral adnexal regions, each lesion was evaluated separately, and its laterality was recorded. When more than two masses were observed within an adnexal region, the mass with the highest score was used for analysis. Therefore, up to two masses per patient were included in the evaluation.

Standard of reference

The standard of reference for adnexal masses was surgical histopathological diagnosis or imaging follow-up by MRI, computed tomography (CT), or US. If imaging follow-up for at least 1 year showed that the mass was stable or decreased in size, it was considered benign. If the mass showed a rapid increase in size accompanying other signs of malignancy (e.g., elevation of tumour markers, abnormal cytology of ascites, or peritoneal implants, lymphadenopathy or metastasis on imaging) or interval regression in size after chemotherapy, it was considered malignant. The standard of reference was assessed by a separate radiologist with 18 years of experience in abdominal imaging who was blinded to the results of the image analysis.

Final diagnoses were established by means of surgical pathologic diagnosis for 662 lesions (481 benign and 181

Table 1
Definitions of imaging features

Term	Definition
Purely cystic mass	Unilocular cyst or hydrosalpinx, both of which have low T1-weighted and high T2-weighted MRI signal intensities, and no internal enhancement.
Purely endometriotic mass	Lesion displaying high T1-weighted signal intensity greater than or equal to that of subcutaneous fat, with shading on T2-weighted MRI images and no internal enhancement.
Purely fatty mass	Lesion displaying high T1-weighted signal intensity that disappeared after fat saturation and displaying no solid tissue.
Wall enhancement	Enhancement of the wall of a cyst.
Solid tissue	Solid tissue comprising thickened irregular septa and/or vegetation, and/or a solid portion (including completely solid mass) that enhances after gadolinium chelate injection. Diffuse wall thickening, normal ovarian stroma, and regular septa are not considered to represent solid tissue.
Thickened irregular septa	Focal areas of septal thickening with thickness ≥3 mm within a cyst.
Vegetations	Solid papillary projections into the cyst from the cyst wall with heights ≥3 mm.
Solid portion	Measurable solid component other than thickened irregular septa or vegetations. This group includes completely solid masses.
T2-weighted signal intensity within solid tissue	Signal intensity defined in comparison with adjacent external myometrium (considered low if T2 signal is lower than and intermediate if T2 signal is equal to or higher than that of outer myometrium).
b=1000 s/mm^2 weighted signal intensity within solid tissue	Signal intensity defined in comparison with serous fluid (cystic bladder or cerebrospinal fluid; considered high if b=1,000 s/mm 2 signal was higher than and low if b=1,000 s/mm^2 signal was equal to or lower than that of serous fluid).
Type 1 time–signal-intensity curve within solid tissue	A gradual increase in the signal intensity of the solid tissue, without a well-defined "shoulder."
Type 2 time–signal-intensity curve within solid tissue	A moderate initial increase in the signal intensity of solid tissue relative to that of myometrium.
Type 3 time–signal-intensity curve within solid tissue	An initial increase in the signal intensity of solid tissue that was steeper than that of myometrium.
Peritoneal implants	Nodular thickening of the peritoneum that enhances after gadolinium chelate injection.

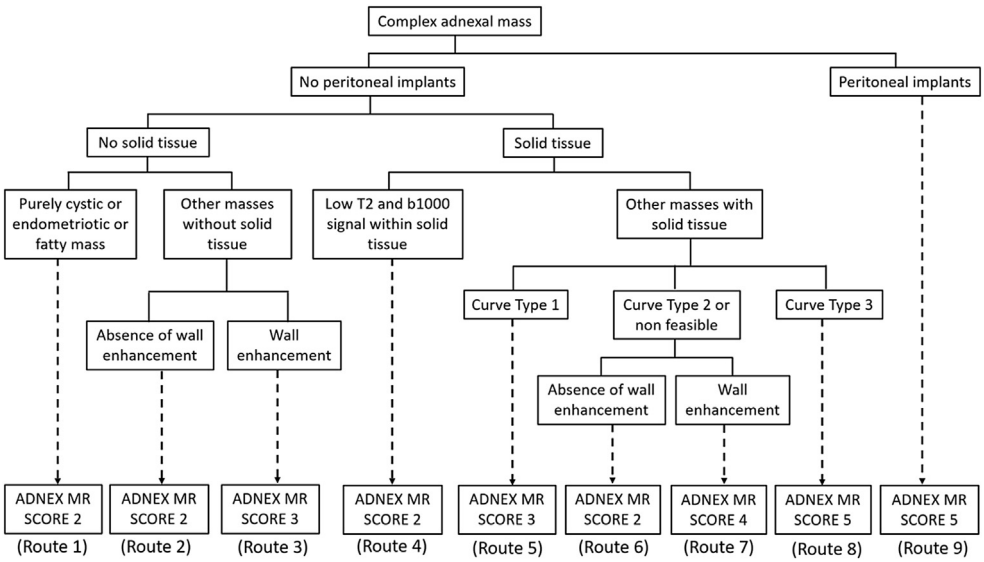

Figure 2 ADNEX MR SCORING system. Non-feasible, no myometrial data were available or there were too many image artefacts. Routes from root node (top of the tree) to each terminal node are numbered from the left.

malignant) and on the basis of imaging follow-up for 116 lesions (109 benign and seven malignant). The interval between MRI and final diagnosis ranged 0 and 2,540 days, with a median of 43 days.

Statistical analysis

Statistical analyses were performed using statistical software (SPSS version 20; SPSS, Chicago, IL, USA). The diagnostic performance of the scoring system for the differentiation of benign and malignant adnexal masses was evaluated by ROC analysis. Borderline epithelial tumours or other tumours of low malignant potential were considered malignant for the analysis. A score of 4 or greater was judged as malignant according to the original report.[6] In addition, the diagnostic accuracy of each individual route in Fig 2 was calculated. The misclassification rate between borderline epithelial tumours or other tumours of low malignant potential and malignant tumours was compared using Fisher's exact test. Inter-reader agreement on the characterisation of the mass (benign versus malignant) was assessed using kappa statistics. A two-tailed p-value of <0.05 was considered to indicate significant difference.

Subgroup analysis

The above-described ROC analysis was performed for a limited number of cases that the readers had not experienced in their clinical settings prior to this study.

Results

The mean patient age was 47.5 years (range 11–89 years). The prevalence rates of malignancy in masses with the ADNEX MR scores of 2, 3, 4 and 5 were 1.9% (8/419), 12.8% (19/149), 62.6% (57/91), and 87.4% (104/119) for reader 1 and 2.1% (9/424), 13.6% (20/147), 67.6% (71/105), and 86.3% (88/102) for reader 2, respectively.

In terms of the differentiation of benign and malignant adnexal masses, the ADNEX MR SCORING system yielded an AUC of 0.929 (95% confidence interval [CI]: 0.908, 0.951) for reader 1 and 0.923 (95% CI: 0.901, 0.946) for reader 2. The sensitivity, specificity and accuracy for the diagnosis of malignancy were 85.6% (161/188; 95% CI: 79.8%, 90.3%), 91.7% (541/590; 95% CI: 89.2%, 93.8%), and 90.2% (702/778; 95% CI: 87.9%, 92.2%) for reader 1 and 84.6% (159/188; 95% CI: 78.6%, 89.4%), 91.9% (542/590; 95% CI: 89.4%, 93.9%) and 90.1% (701/778; 95% CI: 87.8%, 92.1%) for reader 2, respectively.

Inter-reader agreement for the differentiation of masses (benign versus malignant) was excellent, with $\kappa=0.849$ (95% CI: 0.805–0.892).

Table 2 shows the final diagnoses and the number of misclassified cases. Thirty-nine (20.7%) of 188 malignant lesions were borderline epithelial tumours or other tumours of low malignant potential. These lesions had a higher rate of misclassification: 18 (46.1%) of 39 were misclassified by both readers, while nine (6%) and 11 (7.4%) of the other 149 malignant lesions were misclassified ($p<0.01$). Table 3 shows the misclassified cases and their respective routes in Fig 2. Among the routes to the ADNEX MR score of 2 (routes 1, 2, 4, and 6 in Fig 2), route 6 had a relatively high prevalence of malignancy (47.1% and 36.4%; Fig 6). Among the malignant masses misclassified as benign, 8/27 (29.6%) and 9/29 (31%) were misclassified because of a lack of measurable solid tissue (route 3); most of the cases were mucinous tumours, especially the borderline tumours.

Table 4 shows the rate of malignancy in masses with time–signal-intensity curve type 1, 2 and 3, respectively. Eleven (5.9%) of 188 malignant lesions showed weak and gradual enhancement patterns according to both readers' evaluations and were misclassified as benign (route 5). In

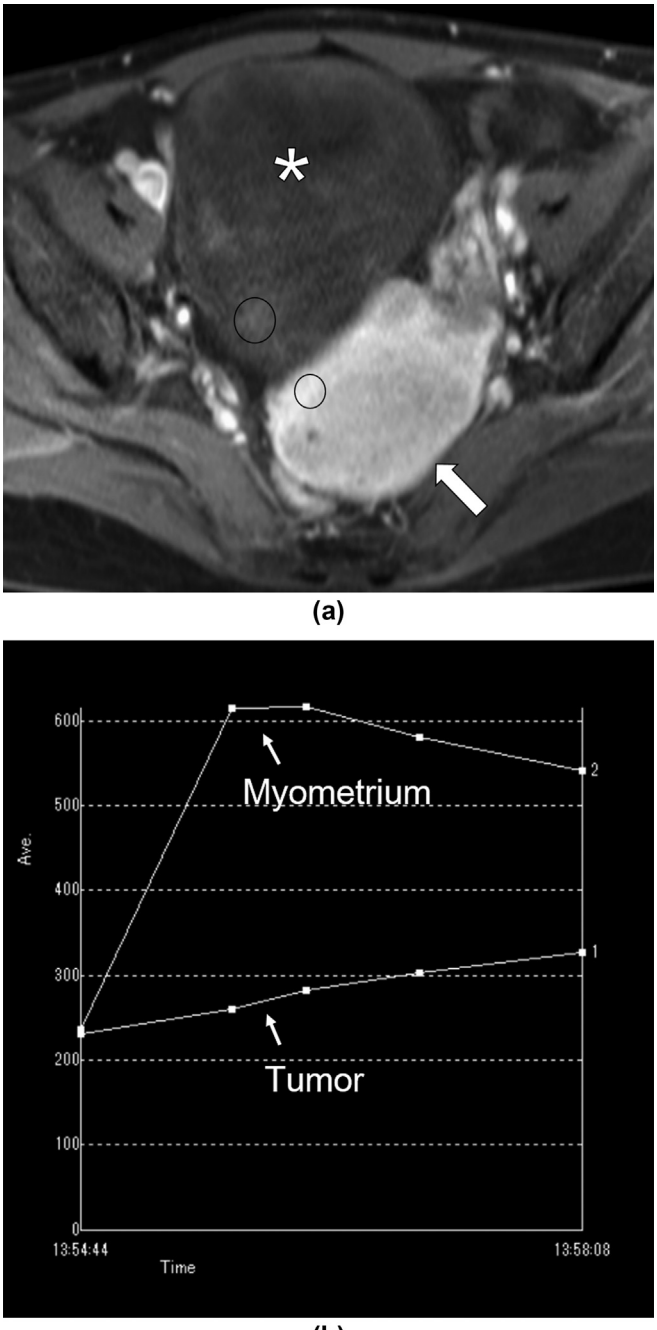

Figure 3 A 48-year-old woman with a fibroma. (a) Axial dynamic contrast-enhanced fat-suppressed T1-weighted images show a completely solid mass (asterisk) anterior to the uterus (arrow). The tumour shows very weak enhancement compared to the uterus. (b) Time–signal intensity curves of the tumour and myometrium. The tumour shows a gradual increase in the signal intensity without a well-defined "shoulder" (curve type 1).

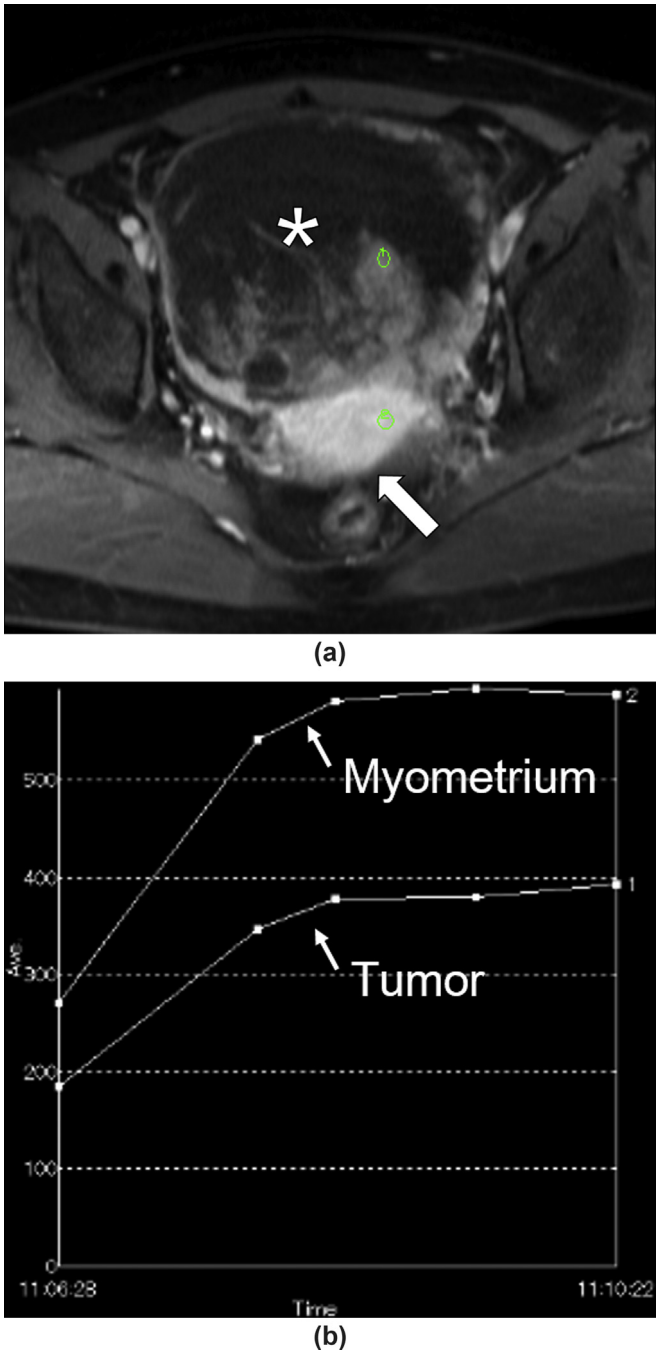

Figure 4 A 74-year-old woman with endometrioid adenocarcinoma. (a) Axial dynamic contrast-enhanced fat-suppressed T1-weighted image shows a heterogeneously enhanced mass (asterisk) anterior to the uterus (arrow). (b) Time–signal intensity curves of the tumour and myometrium. The tumour shows a moderate initial increase in the signal intensity relative to that of the myometrium (curve type 2).

contrast, 15 (2.5%; reader 1) and 16 (2.7%; reader 2) of 590 benign masses were misclassified as malignant because they had solid tissue with a rapid and strong enhancement pattern (route 8).

Masses with peritoneal implants were always classified as malignant (route 9) by both readers; more than half of the cases were serous carcinomas (63.6% [35/55] and 60% [30/50] by readers 1 and 2, respectively).

Readers 1 and 2 had experience with 250 patients with 288 masses (37% of all masses) and 69 patients with 89 masses (11.4%) in their respective clinical settings prior to this study. Even after these patients were excluded, their diagnostic performance was still excellent, with an AUC of

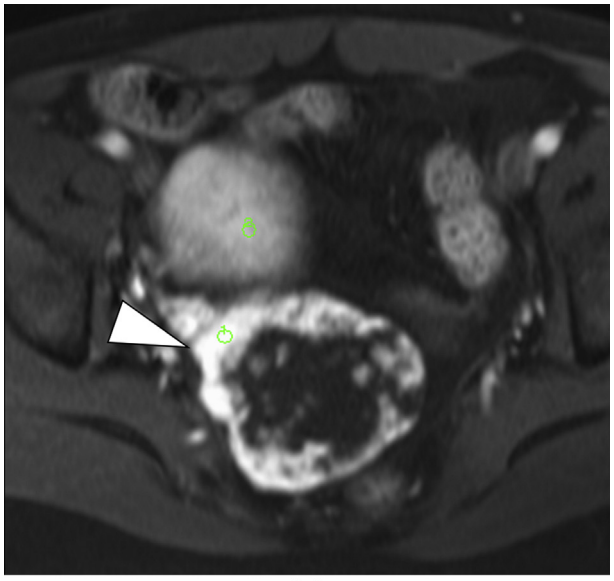

(a)

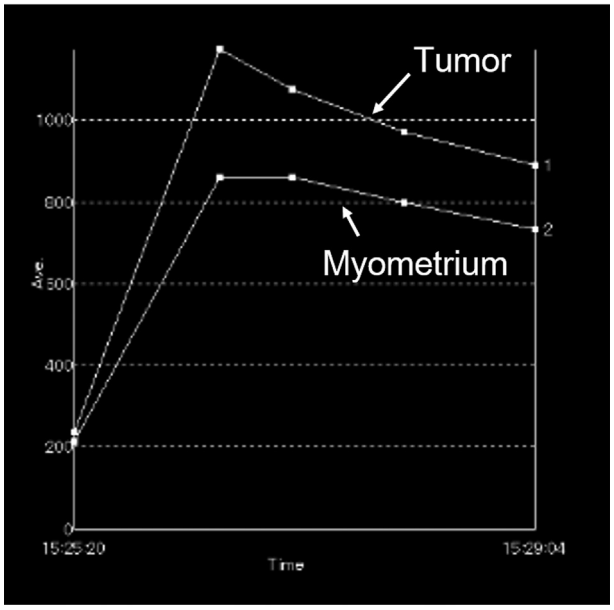

(b)

Figure 5 A 21-year-old woman with a sclerosing stromal tumour. (a) Axial dynamic contrast-enhanced fat-suppressed T1-weighted image shows very intense enhancement of the periphery of the tumour (arrowhead). (b) Time–signal intensity curves of the tumour and myometrium. The tumour shows a steeper initial increase in the signal intensity compared to that of the myometrium (curve type 3).

0.933 (95% CI: 0.913, 0.953) for reader 1 and 0.928 (95% CI: 0.906, 0.949) for reader 2.

Discussion

The present study showed that the ADNEX MR SCORING system proposed by Thomassin- Naggara *et al.*[6] had an excellent diagnostic performance in differentiating benign and malignant adnexal masses in the external population. The AUCs of 0.929 and 0.923 in this study were similar to that found in another external validation study by Ruiz *et al.* (AUC of 0.92).[7]

Peritoneal implants are the first imaging feature to be evaluated in the ADNEX MR SCORING system. In the present population, all cases with peritoneal implants were malignant.

The presence or absence of solid tissue (vegetation, a solid portion, and irregular thickened septa) within an

Table 2
Details of the standard of reference.

Final diagnosis	Number of masses	Misclassified cases	
		Reader 1	Reader 2
Benign			
Endometrioma	167	8 (4.8)	9 (5.4)
Serous cystadenoma	50	2 (4)	2 (4)
Serous adenofibroma	2	1 (50)	1 (50)
Mucinous cystadenoma	58	2 (3.4)	3 (5.2)
Brenner tumour	1	0	0
Fibroma	14	0	0
Thecoma	12	3 (25)	3 (25)
Sclerosing stromal tumour	1	1 (100)	1 (100)
Mature teratoma	132	17 (12.9)	10 (7.6)
Struma ovarii	5	3 (60)	3 (60)
Benign cyst (eg, paraovarian cyst, peritoneal inclusion cyst, lymphangioma)	16	0	1 (6.3)
Functional	3	0	0
Tubo-ovarian abscess	5	4 (80)	3 (60)
Adnexal torsion	2	0	0
Hydro-/haematosalpinx	2	0	0
Myoma	9	3 (33.3)	2 (22.2)
Pelvic uterus-like mass	1	1 (100)	1 (100)
Foreign body granuloma	1	1 (100)	1 (100)
Benign mass by imaging follow-up	109	3 (2.8)	8 (7.3)
Total	590	49 (8.3)	48 (8.1)
Malignant			
Serous borderline tumour[a]	8	2 (25)	1 (12.5)
Mucinous borderline tumour[a]	17	8 (47.1)	10 (58.8)
Clear cell borderline tumour[a]	1	1 (100)	1 (100)
Seromucinous borderline tumour[a]	1	0	0
Serous carcinoma	52	1 (1.9)	2 (3.8)
Mucinous carcinoma	9	3 (33.3)	2 (22.2)
Endometrioid carcinoma	20	2 (10)	2 (10)
Clear cell carcinoma	27	1 (3.7)	2 (7.4)
Other ovarian carcinoma (neuroendocrine, adenosquamous, unclassified)	7	0	0
Immature teratoma[a]	1	0	0
Malignant transformation of mature teratoma	3	0	1 (33.3)
Yolk sac tumour	1	0	0
Granulosa cell tumour[a]	6	4 (66.7)	3 (50)
Sertoli–Leydig cell tumour[a]	3	2 (66.7)	2 (66.7)
Sex cord–stromal tumour, unclassified[a]	1	0	0
Metastasis	13	2 (15.4)	2 (15.4)
Tubal carcinoma	2	0	0
Peritoneal carcinoma	3	0	0
Malignant mesothelioma	1	0	0
Sarcoma	3	0	0
Wolffian tumour[a]	1	1 (100)	1 (100)
Malignant lymphoma	1	0	0
Malignant mass by imaging follow-up	7	0	0
Total	188	27 (14.4)	29 (15.4)

Data are numbers of lesions with percentages in parenthesis.
[a] Borderline epithelial tumours or other tumours of low malignant potential.

Table 3
Misclassified cases in the ADNEX MR SCORING system.

ADNEX MR score	Route[a]	Reader 1		Reader 2	
		Misclassified cases[b]	Final diagnosis of misclassified cases	Misclassified cases[a]	Final diagnosis of misclassified cases
2: Benign mass	1	0/374 (0) [0, 0.8]		1/374 (0.3) [0, 1.5]	Malignant transformation of mature teratoma 1
	2	0/8 (0) [0, 31.2]		0/14 (0) [0, 19.3]	
	4	0/20 (0) [0, 13.9]		0/14 (0) [0, 19.3]	
	6	8/17 (47.1) [27.8, 77]	Granulosa cell tumour 2, Sertoli–Leydig cell tumour 2, metastasis 2, clear cell borderline tumour 1, Wolffian tumour 1	8/22 (36.4) [17.2, 59.3]	Granulosa cell tumour 2, Sertoli–Leydig cell tumour 2, metastasis 2, clear cell borderline tumour 1, serous carcinoma 1
3: Probably benign mass	3	8/101 (7.9) [3.5, 15]	Mucinous borderline tumour 5, mucinous carcinoma 1, endometrioid carcinoma 1, granulosa cell tumour 1	9/94 (9.6) [4.5, 17.4]	Mucinous borderline tumour 7, mucinous carcinoma 1, endometrioid carcinoma 1
	5	11/48 (22.9) [12, 37.3]	Mucinous borderline tumour 3, mucinous carcinoma 2, serous borderline tumour 2, serous carcinoma 1, endometrioid carcinoma 1, clear cell carcinoma 1, granulosa cell tumour 1	11/53 (20.8) [10.8, 34.1]	Mucinous borderline tumour 3, clear cell carcinoma 2, mucinous carcinoma 1, serous borderline tumour 1, serous carcinoma 1, endometrioid carcinoma 1, granulosa cell tumour 1, Wolffian tumour 1
4: Indeterminate mass	7	34/85 (40) [29.5, 51.2]	Mature teratoma 15, endometriotic cyst 7, benign mucinous tumour 2, thecoma 2, myoma 2, benign mass by imaging follow-up 2, benign serous tumour 2, pelvic uterus-like mass 1, foreign body granuloma 1	34/105 (32.4) [23.6, 42.2]	Endometriotic cyst 9, mature teratoma 8, benign mass by imaging follow-up 6, benign mucinous tumour 2, thecoma 2, benign serous tumour 2, benign cyst 1, tubo-ovarian abcess 1, myoma 1, pelvic uterus-like mass 1, foreign body granuloma 1
5: Probably malignant mass	8	15/64 (23.4) [13.8, 35.7]	Tubo-ovarian abscess 4, struma ovarii 3, mature teratoma 2, serous adenofibroma 1, endometriotic cyst 1, thecoma 1, sclerosing stromal tumour 1, myoma 1, benign mass by imaging follow-up 1	14/52 (26.9) [15.6, 41]	Struma ovarii 3, mature teratoma 2, tubo-ovarian abscess 2, benign mass by imaging follow-up 2, serous adenofibroma 1, endometriotic cyst 1, thecoma 1, sclerosing stromal tumour 1, myoma 1,
	9	0/55 [0, 5.3]		0/50 (0) [0, 5.8]	

[a] Routes are shown in Fig 2.
[b] Data are numbers of lesions with percentages in parentheses and 95% confidence intervals in brackets.

adnexal mass is the next imaging feature to be evaluated. Any masses without solid tissue are classified as benign (scored 2 or 3) in the ADNEX MR SCORING system. In general, a cystic mass without solid tissue is suggestive of benignity.[9] Thomassin- Naggara *et al.* have reported that the absence of solid tissue is highly predictive of benignity (positive likelihood ratio of malignancy=0.08).[6] In the present population, cystic or fatty masses with a score of 2 (route 1) showed an extremely low prevalence of malignancy (0% and 0.3% for readers 1 and 2, respectively); however, the cystic masses with a score of 3 (route 3), encompassing masses other than purely cystic, endometriotic, or fatty masses that have wall enhancement, showed a higher prevalence of malignancy (7.9% [8/101] and 9.6% [9/94] for readers 1 and 2) compared to the original study (4.3% [3/70]). Most of these cases were mucinous borderline tumours. The common appearance of a mucinous borderline tumour is a multilocular cystic mass with numerous and thickened septa.[10,11] Mucinous ovarian tumours are thought to represent a stepwise tumour progression akin to the adenoma–carcinoma sequence in colorectal cancer[12] and the morphological appearance of borderline tumours is between their benign and malignant counterparts.[13,14] Therefore, although some differences in imaging features between borderline and benign mucinous tumours have been reported,[15] borderline tumours are often difficult to differentiate from benign tumours.

An adnexal mass with solid tissue is usually considered malignant[9,14]; however, some benign adnexal masses can have solid tissue. Ovarian fibroma or thecoma, or leiomyoma (pedunculated uterine or within a broad ligament) are common benign adnexal masses that are predominantly solid.[2,13,16] Other benign masses including ovarian cystadenoma with thick septa or vegetation, cystadenofibroma, haemorrhagic cyst or endometrioma, granulomatous salpingo-oophoritis, mature cystic teratoma or struma ovarii can be false positives for malignancy.[1,17–22] Thomassin-Naggara *et al.* reported that the presence of solid tissue is not sufficient to predict malignancy (positive likelihood ratio of malignancy=4.38).[6] In fact, solid tissue was observed in 19.5% (115/590) and 23.2% (137/590) of benign masses in the present population by readers 1 and 2, respectively.

Therefore, solid tissue within an adnexal mass should be further characterised to differentiate benign from malignant masses; the combination of signal intensity on T2-

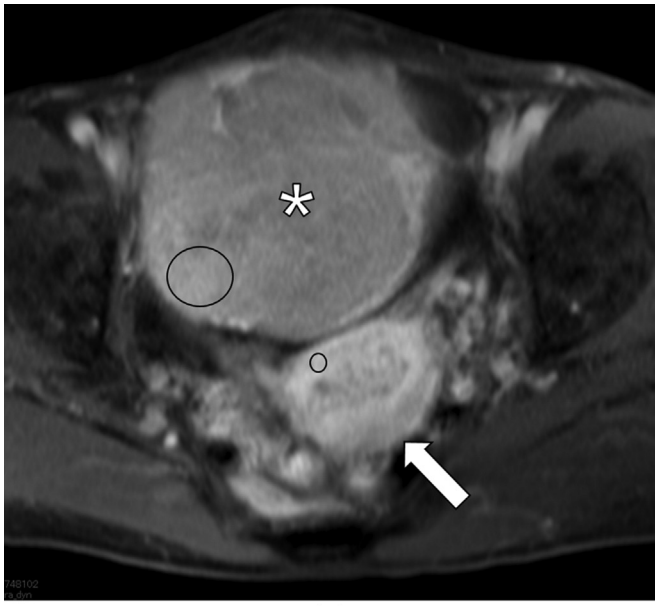

(a)

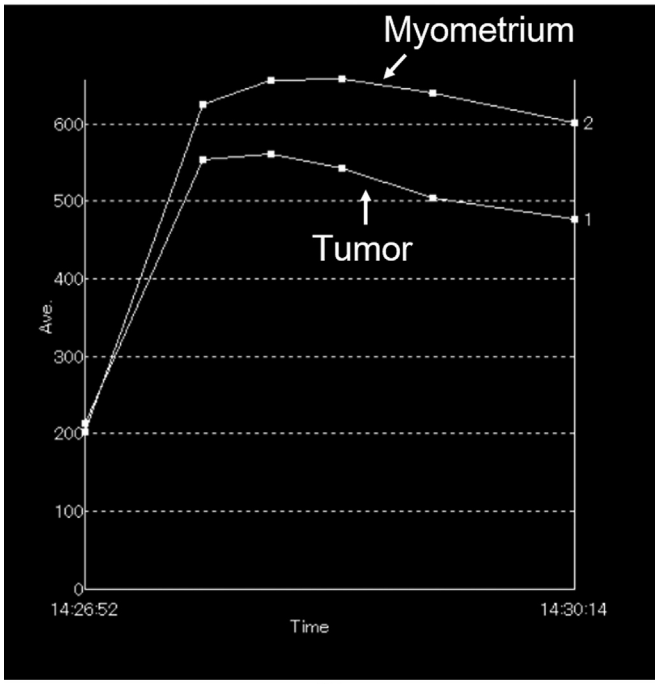

(b)

Figure 6 A 62-year-old woman with a Sertoli–Leydig cell tumour of low malignant potential. (a) Axial dynamic contrast-enhanced fat-suppressed T1-weighted image shows a completely solid mass without wall enhancement (asterisk) anterior to the uterus (arrow). (b) Time–signal intensity curves of the tumour and myometrium. The tumour shows a moderate initial increase in the signal intensity relative to that of the myometrium (curve type 2). The mass was scored as 2 by both readers.

weighted and DWI, and the time–signal-intensity curve on perfusion WI are the key findings in making this differentiation in the ADNEX MR SCORING system.

An adnexal mass with solid tissue that simultaneously displays low signal intensity on T2-weighted and on b=1,000 DWI images is categorised as benign (with a score of 2); the masses in which this finding was made in the present population were always benign, as in the original report.[6]

Table 4
Rate of malignancy in masses with time–signal-intensity curve type 1, 2 and 3.

Reader	Time-signal-intensity curves		
	Type 1	Type 2[a]	Type 3
1	11/48 (22.9)	54/85 (63.5)	49/64 (76.6)
2	11/53 (20.8)	68/97 (70.1)	36/52 (69.2)

Data are numbers of malignant lesions with percentages in parentheses.
[a] Masses without wall enhancement (route 6 in Fig 2) and non-feasible cases in route 7 are excluded.

Other solid tissues are to be classified into three categories by time–signal intensity curves on perfusion WI. In epithelial ovarian tumours, the curve types 1, 2 and 3 are suggestive of benign, borderline, and invasive tumours, respectively.[23] The classification of adnexal masses by these curves led to more overlaps between benign and malignant diagnoses in the present study than in the original study.[6] The prevalence rates of malignancy in masses with curve type 1 were 22.9% (11/48) and 20.8% (11/53) in the present study while this rate was 5% (1/22) in the original study. The prevalence rates of benignity in masses with curve type 3 were 23.4% (15/64) and 30.1% (16/52) in the present study, while this rate was 0% (0/14) in the original study. An explanation for these discrepancies might be the lower temporal resolution on dynamic contrast-enhanced study in the present protocol; images were obtained at 30-second intervals in the present protocol but at 2.4-second intervals in the original study. The lower temporal resolution might have decreased accuracy in assessing the initial peak of the time–signal-intensity curve as reported in a study on prostate cancer.[24]

Adnexal masses with curve type 2 solid tissue are divided by the presence or absence of wall enhancement; the absence of wall enhancement is given a score of 2 and the presence of wall enhancement is given a score of 4; however, the former included 36.4%–47.1% of malignancies in the present population but 0% in the original study. The above-mentioned difference in temporal resolution on the dynamic contrast-enhanced study might be a cause of the discrepancy.

There are limitations to this study. First, the MRI images were reviewed retrospectively, and the readers had previous experience with some members of the study population. Although the diagnostic performance was almost the same after these patients were excluded, recall bias may have affected the results. Second, as noted above, the lower time resolution on the dynamic contrast-enhanced study might have decreased the accuracy of the stratification for the risk of malignancy based on the curves. Third, not all patients were diagnosed by histopathological evaluation. Final diagnoses based on imaging follow-up might have resulted in misclassification. For example, even malignant tumours, especially low-grade or borderline tumours, can be stable in size for long periods. Fourth, although the present study population was made up of patients with

indeterminate adnexal masses upon US, the examinations were performed by many gynaecologists with various levels of experience, and the referral pattern for MRI might have differed among these practitioners; however, the excellent diagnostic performance in this study supports the generalisability of the ADNEX MR SCORING system. Fifth, the learning curve with the ADNEX MR scoring system was not evaluated, nor did were the differences in diagnostic performance among readers with various levels of experience assessed in the interpretation of MRI examinations of indeterminate adnexal masses.

In conclusion, the ADNEX MR SCORING system was highly accurate in differentiating benign and malignant adnexal masses, although it may be less accurate for borderline epithelial tumours or other tumours of low malignant potential.

Conflict of interest

The authors declare no conflict of interest.

References

1. Sohaib SA, Sahdev A, Van Trappen P, *et al*. Characterization of adnexal mass lesions on MRI. *AJR Am J Roentgenol* 2003;**180**:1297–304.
2. Spencer JA, Forstner R, Cunha TM, *et al*. ESUR Female Imaging Sub-Committee. ESUR guidelines for MRI of the sonographically indeterminate adnexal mass: an algorithmic approach. *Eur Radiol* 2010;**20**:25–35.
3. Hricak H, Chen M, Coakley FV, *et al*. Complex adnexal masses: detection and characterization with MRI—multivariate analysis. *Radiology* 2000;**214**:39–46.
4. Thomassin-Naggara I, Daraï E, Cuenod CA, *et al*. Dynamic contrast-enhanced magnetic resonance imaging: a useful tool for characterizing ovarian epithelial tumours. *J Magn Reson Imaging* 2008;**28**:111–20.
5. Thomassin-Naggara I, Daraï E, Cuenod CA, *et al*. Contribution of diffusion-weighted MRI for predicting benignity of complex adnexal masses. *Eur Radiol* 2009;**19**:1544–52.
6. Thomassin-Naggara I, Aubert E, Rockall A, *et al*. Adnexal masses: development and preliminary validation of an MRI scoring system. *Radiology* 2013;**267**:432–43.
7. Ruiz M, Labauge P, Louboutin A, *et al*. External validation of the MRI scoring system for the management of adnexal masses. *Eur J Obstet Gynecol Reprod Biol* 2016;**205**:115–9.
8. Thomassin-Naggara I. EURAD-MR Classification: European Multicenter Study (EURAD). Available at: https://clinicaltrials.gov/ct2/show/NCT01738789. Accessed 29 May 2018.
9. Valentini AL, Gui B, Miccò M, *et al*. Benign and suspicious ovarian masses—MRI criteria for characterization: pictorial review. *J Oncol* 2012;**2012**:481806.
10. Bazot M, Haouy D, Daraï E, *et al*. Is MRI a useful tool to distinguish between serous and mucinous borderline ovarian tumours? *Clin Radiol* 2013;**68**:e1–8.
11. Bent CL, Sahdev A, Rockall AG, *et al*. MRI appearances of borderline ovarian tumours. *Clin Radiol* 2009;**64**:430–8.
12. Lalwani N, Shanbhogue AK, Vikram R, *et al*. Current update on borderline ovarian neoplasms. *AJR Am J Roentgenol* 2010;**194**:330–6.
13. Foti PV, Attinà G, Spadola S, *et al*. MRI of ovarian masses: classification and differential diagnosis. *Insights Imaging* 2016;**7**:21–41.
14. Sohaib SA, Reznek RH. MRI in ovarian cancer. *Cancer Imaging* 2007;**7**:S119–29.
15. Zhao SH, Qiang JW, Zhang GF, *et al*. MRI in differentiating ovarian borderline from benign mucinous cystadenoma: pathological correlation. *J Magn Reson Imaging* 2014;**39**:162–6.
16. Iyer VR, Lee SI. MRI, CT, and PET/CT for ovarian cancer detection and adnexal lesion characterization. *AJR Am J Roentgenol* 2010;**194**:311–21.
17. Bazot M, Nassar-Slaba J, Thomassin-Naggara I, *et al*. MRI compared with intraoperative frozen-section examination for the diagnosis of adnexal tumours; correlation with final histology. *Eur Radiol* 2006;**16**:2687–99.
18. Fenchel S, Grab D, Nuessle K, *et al*. Asymptomatic adnexal masses: correlation of FDG PET and histopathologic findings. *Radiology* 2002;**223**:780–8.
19. Stevens SK, Hricak H, Stern JL. Ovarian lesions: detection and characterization with gadolinium-enhanced MRI at 1.5 T. *Radiology* 1991;**181**:481–8.
20. Yamashita Y, Torashima M, Hatanaka Y, *et al*. Adnexal masses: accuracy of characterization with transvaginal US and precontrast and postcontrast MRI. *Radiology* 1995;**194**:557–65.
21. Balan P. Ultrasonography, computed tomography and magnetic resonance imaging in the assessment of pelvic pathology. *Eur J Radiol* 2006;**58**:147–55.
22. Kawahara K, Yoshida Y, Kurokawa T, *et al*. Evaluation of positron emission tomography with tracer 18-fluorodeoxyglucose in addition to magnetic resonance imaging in the diagnosis of ovarian cancer in selected women after ultrasonography. *J Comput Assist Tomogr* 2004;**28**:505–16.
23. Thomassin-Naggara I, Bazot M, Daraï E, *et al*. Epithelial ovarian tumours: value of dynamic contrast-enhanced MRI and correlation with tumour angiogenesis. *Radiology* 2008;**248**:148–59.
24. Othman AE, Falkner F, Weiss J, *et al*. Effect of temporal resolution on diagnostic performance of dynamic contrast-enhanced magnetic resonance imaging of the prostate. *Invest Radiol* 2016;**51**:290–6.